Ridaifen-G Induces Caspase-independent Atypical Cell Death

Anniwaer Anlifeire[1,2], Manami Hatori[2], Akinori Morita[2], Isamu Shiina[3], Kenya Nakata[3], Yu-Ta Tosaki[3], Yan-Wen Wang[3], Masahiko Ikekita[2], Guan Li[1]*

([1]*College of Life Science, Xinjiang University, Urumqi 830046, China*; [2]*Department of Applied Biological Science, Faculty of Science and Technology, Chiba-ken 278-8510, Japan*; [3]*Department of Applied Chemistry, Faculty of Science, Tokyo University of Science, Tokyo 162-8601, Japan*)

Abstract We have investigated antitumor activities of Ridaifens (RIDs), which are a series of synthesized Tamoxifen (TAM) derivatives. In this study, we focused on one of RIDs, Ridaifen-G (RID-G), and investigated the cell death-inducing activity of it in four neoplastic hematopoietic cell lines, U937, Raji, THP-1, and IM-9 cells in the presence or absence of a pan-caspase inhibitor, Z-VAD-fmk. The aim of this study is to characterize the mode of RID-G-induced cell death, as compared with a typical apoptosis of etoposide-treated U937 cells, which die mainly through mitochondria-mediated apoptotic pathway in a caspase-dependent manner. To obtain reliable results, we analyzed RID-G-induced cell death by four methods, i.e., MTT assay, MitoTracker staining, AnnexinV-FITC/Propidium Iodide double staining, and DNA ladder formation. These analyses revealed that RID-G-induced cell death is accompanied by mitochondrial dysfunction and executed in a caspase-independent manner except DNA ladder formation. Z-VAD-fmk did not suppress the death, but suppressed etoposide-induced apoptosis in U937 cells. In DNA ladder formation analysis, RID-G induced a smear of DNA fragmentation in Raji and THP-1 cells, and RID-G-treated U937 cells showed less DNA ladder formation than when treated with etoposide. In addition, Z-VAD-fmk showed different effects on these DNA fragmentations: it largely suppressed, partialy suppressed, and on the contrary, enhanced DNA fragmentaion in U937, THP-1, and Raji cells, respectively. These results suggest that RID-G induces caspase-independent atypical cell death, which is accompanied by mitochondrial dysfunction.

Key words cell death; mitochondria; caspase; apoptosis; Ridaifen-G

Apoptosis, or programmed cell death, is a normal component of the development and health of multicellular organisms. Cells die in response to a variety of stimuli and during apoptosis they do so in a controlled, regulated fashion. This makes apoptosis distinct from another form of cell death called necrosis in which uncontrolled cell death leads to lysis of cells, inflammatory responses and, potentially, to serious health problems. Apoptosis, by contrast, is a process in which cells play an active role in their own death (which is why apoptosis is often referred to as cell suicide).

Mitochondria play an important role in the regulation of apoptosis(Fig.1). With multiple cytotoxic stimuli, including UV, X-ray, and many chemical drugs, mitochondrial perturbation occurs by mitochondrial membrane potential ($\Delta\Psi_m$) reduction and cytochrome *c* (Cyt *c*) release into the cytosol[1,2]. Bcl-2 family proteins are involved in the stability of the mitochondrial membrane by promoting or preventing mitochondrial perturbation[3~5]. When mitochondrial stability is attenuated, released Cyt *c* binds to the cytosolic adaptor protein, apoptotic protease activating factor-1 (Apaf-1), and the complex activates one of the initiator caspases, caspase-9[6]. Activated caspase-9 in turn activates the effector caspases (caspase-3, -6, and -7) to implement apoptosis by means of chromatin DNA fragmentation, morphological changes, and cell-volume loss. Overall,

Received: January 19, 2011 Accepted: March 3, 2011

*Corresponding author. Tel: 86-991-8581106, E-mail: guanli@xju.edu.cn

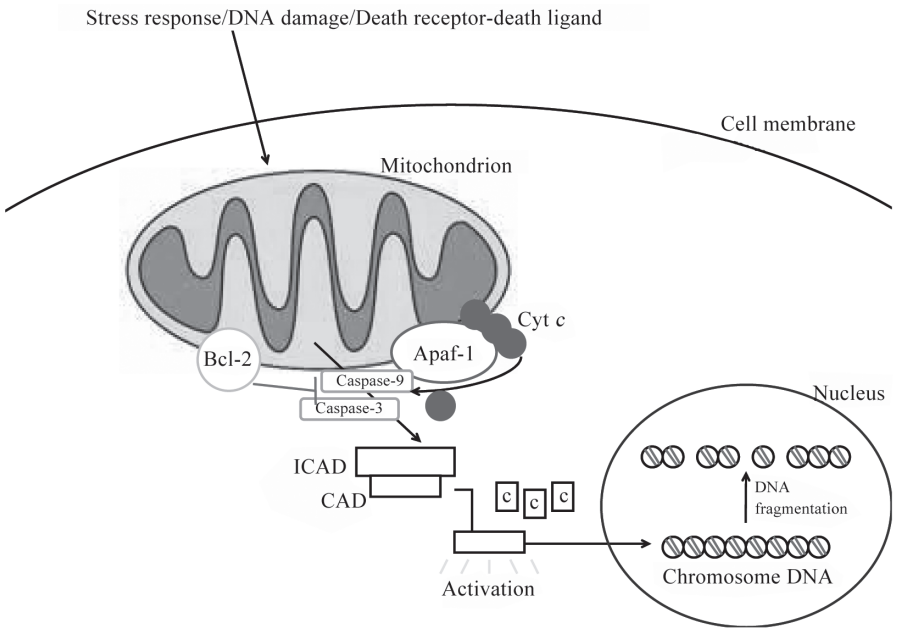

Fig.1 Role of mitochondria in apoptosis

mitochondrial perturbation tends to induce apoptosis. However, mitochondria participated in TAM-induced apoptosis is not clear. Mandlekar[7] discovered that caspase-9 is slightly activated during TAM-induced apoptosis, suggesting mitochondrial participation. In contrast, Ferlini[8] has reported that mitochondria-localized anti-apoptotic protein Bcl-2 expression and functional inactivation by phosphorylation is unchanged during TAM-induced apoptosis, assuming that TAM-induced apoptosis is independent of mitochondria.

We have recently developed a rapid synthesis of pseudo-symmetrical TAM derivatives, Ridaifens (RIDs)[9~13]. RIDs can be synthesized as novel analogues of TAM, and one of RIDs, Ridaifen-B (RID-B) shows more potent apoptosis-inducing activity than the original TAM[9]. In the present study, we focused on a conformational analog of RID-B, RID-G, and investigated the cell death-inducing activity of it in several neoplastic hematopoietic cell lines. Our cell death analyses by four methods in the presence or absence of a pan-caspase inhibitor, Z-VAD-fmk, revealed that RID-G-induced cell death is accompanied by mitochondrial dysfunction in a caspase-independent manner.

1 Materials and Methods

1.1 Cell culture and treatment

The human monoblastic lymphoma cell line U937, the human multiple myeloma cell line IM-9, the human Burkitt's lymphoma cell line Raji, and the human acute monocytic leukemia cell line THP-1 were cultured in RPMI 1640 medium (Wako, Japan) supplemented with 10% fetal bovine serum (FBS, Gibco, USA). Cells were maintained at 37 °C in a humidified atmosphere containing 5% CO_2. Cells were counted with a cell counter (Z1 Cell and particle counter, Beckman Coulter, USA). RID-G was chemically synthesized in our laboratory at Tokyo University of Science (Fig.2)[10~13]. Etoposide and Z-VAD-FMK were purchased from Wako and Peptide Institute (Japan), respectively. These agents were dissolved in dimethyl sulfoxide at stock concentrations of 10 mmol/L. Cells were seeded into plates or flasks (Becton Dickinson, USA) at concentrations of 2×10^5 cells/ml unless otherwise specified, and preincubated at 37 °C for 18 h. The cells were then treated with 5 μmol/L RID-G, and U937 cells were also treated with 5 μmol/L etoposide for indicated periods in the presence or absence of 20 μmol/L Z-VAD-fmk. Z-VAD-fmk was added to the

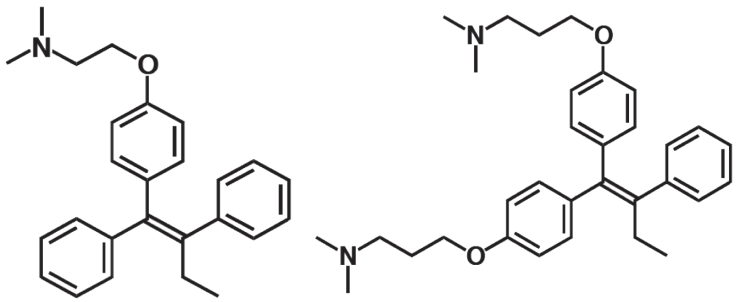

Fig.2 Chemical structures of tamoxifen and its derivative RID-G

culture medium immediately before RID-G or etoposide treatment.

1.2 MTT assay

After the chemical treatments described above, cell viability was determined by MTT assay[14,15], a method for determining cell viability by measuring the mitochondrial dehydrogenase activity. In this assay, 11 μl of MTT stock solution (5 mg/ml in phosphate-buffered saline (PBS)) was added to each well in a 96-well plate (Becton Dickinson), and the plate was incubated at 37 °C for 1 h. After centrifugation for 5 min at 1 500 r/min, the supernatant was discarded, and 100 μl of DMSO was added to each well to dissolve MTT formazan. Absorbance at 570 nm was measured with a microplate reader (Model 550, Bio-Rad, USA), and the cell viabilities were defined as the percentage of the absorbance values compared with the absorbance value of vehicle-treated control[15].

1.3 Flow cytometric analysis

For each sample, 10 000 cells were analyzed with a flow cytometer (FACS Calibur, Becton Dickinson)[16]. The percentage of cell death was determined by Annexin V-FITC and Propidium Iodide (PI) double staining using a MEBCYTO Apoptosis Kit (MBL, Japan) according to the manufacturer's instructions. Early stage cell death was defined as the percentage of Annexin V-positive and PI-negative cells, and late stage cell death was defined as the percentage of Annexin V/PI-double positive cells. The percentage of cells losing their $\Delta\Psi_m$ was determined by MitoTracker staining. After the treatments, cells were incubated in culture medium for 30 min at 37 °C with 100 nmol/L MitoTracker Red CMXRos dye (Invitorgen, USA). The cells were then washed twice, suspended in ice-cold PBS, and analyzed by flow cytometer.

1.4 DNA fragmentation analysis

The chemical treatments in this analysis were performed at cell densities of 8×10^5 cells/ml. For DNA extraction, 1×10^6 cells were suspended in 200 μl of PBS, and lysed by adding 50 μl of lysis buffer (50 mmol/L EDTA-NaOH, pH8.0, 3% Sarkosyl), and 50 μl of RNase A (10 mg/ml) for 2 h at 56 °C followed by 30 μl of proteinase K (10 mg/ml in PBS) overnight incubation at 56 °C. Cellular genomic DNAs were then extracted from the lysates by phenol-chloroform extractions, and 70% ethanol precipitation. Aliquots of 2 μg of cellular DNA were separated by electrophoresis on a 1.5% agarose gel, and stained with 1 μg/ml ethidium bromide and visualized under UV light.

2 Results

2.1 RID-G-induced cell death is accompanied by mitochondrial dysfunction

In the process of apoptosis, mitochondrial disruption occurs, resulting in the decrease of mitochondrial dehydrogenase activity and the loss of $\Delta\Psi_m$. To detect whether these events are induced by RID-G, we analyzed the effects of RID-G on four neoplastic hematopoietic cell lines by MTT assay and MitoTracker staining. As shown in Figure 3 and Figure 4, these

analyses showed that RID-G induced mitochondrial dysfunction. In MTT assay (Fig.3), approximately 85% decrease in cell viability was detected in U937, THP-1, and Raji cells by RID-G or etoposide treatment, and IM-9 cells showed a relative resistance to RID-G (50% decrease). In addition, IC_{50} values of U937, IM-9, THP-1, and Raji cells in MTT assay at 8 h after RID-G treatment were 3.2 μmol/L, 7.0 μmol/L, 2.6 μmol/L, and 2.3 μmol/L, respectively (data not shown). Therefore, we used U937, THP-1, and Raji cells as RID-G-sensitive cell lines, and IM-9 cells were used as a relatively resistant cell line.

In MitoTracker staining analysis (Fig.4), these cell lines showed similar sensitivities to RID-G as that observed in MTT assay, since U937, THP-1, and Raji cells were highly sensitive (approximately

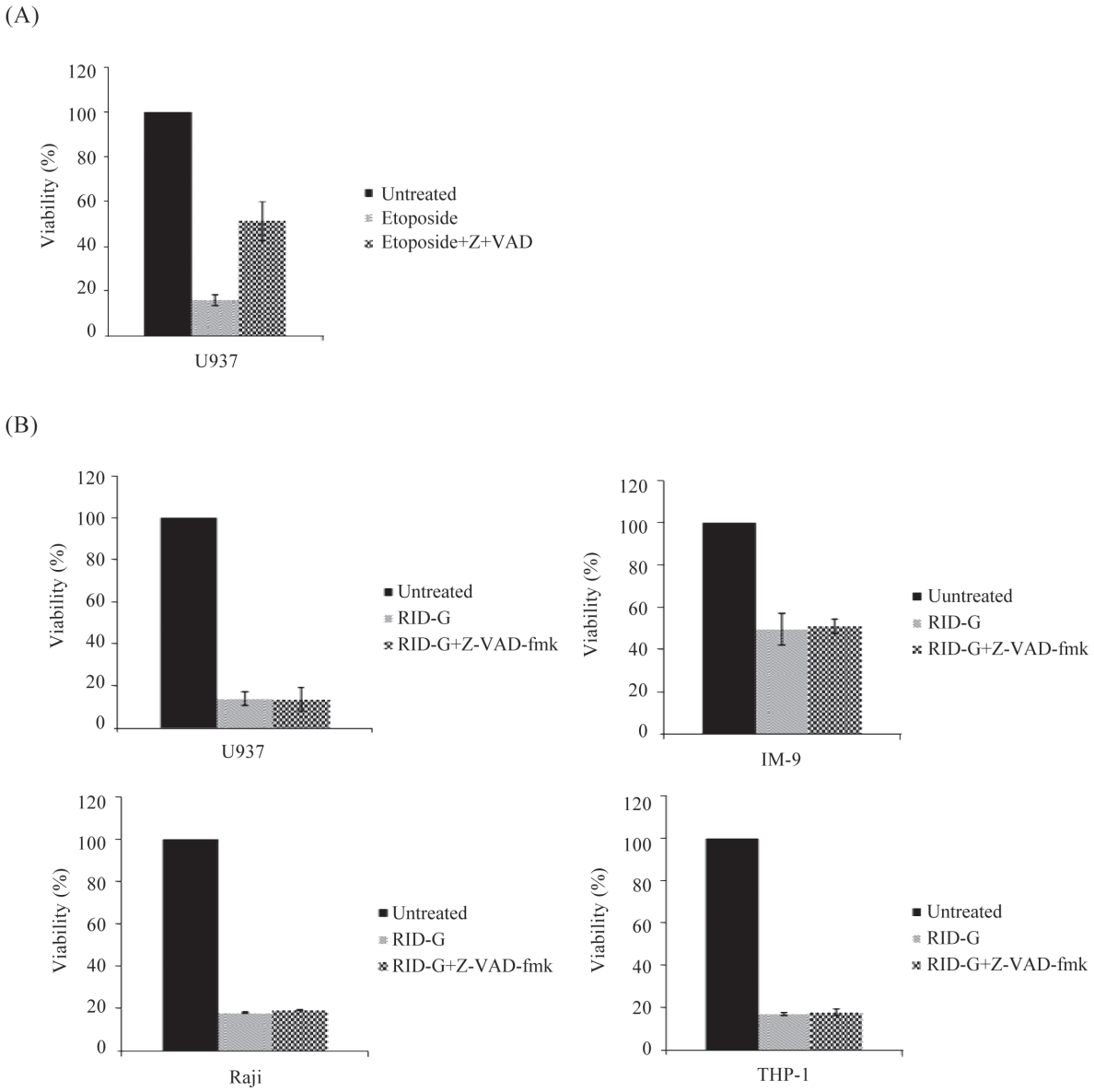

Fig.3 Effects of Z-VAD-fmk on RID-G or etoposide-induced cell death determined by MTT assay

RID-G, etoposide, and Z-VAD-fmk were used at final concentrations of 5 μmol/L, 5 μmol/L, and 20 μmol/L, respectively. The cell viabilities quantified by MTT assay were determined at 4 h (RID-G) or 18 h (etoposide) after treatment. Data shown were means±SD from 3 independent experiments. A: Z-VAD-fmk suppresses etoposide-induced cell death in U937 cells; B: Z-VAD-fmk can not suppress RID-G-induced cell death in U937, IM-9, THP-1, and Raji cells.

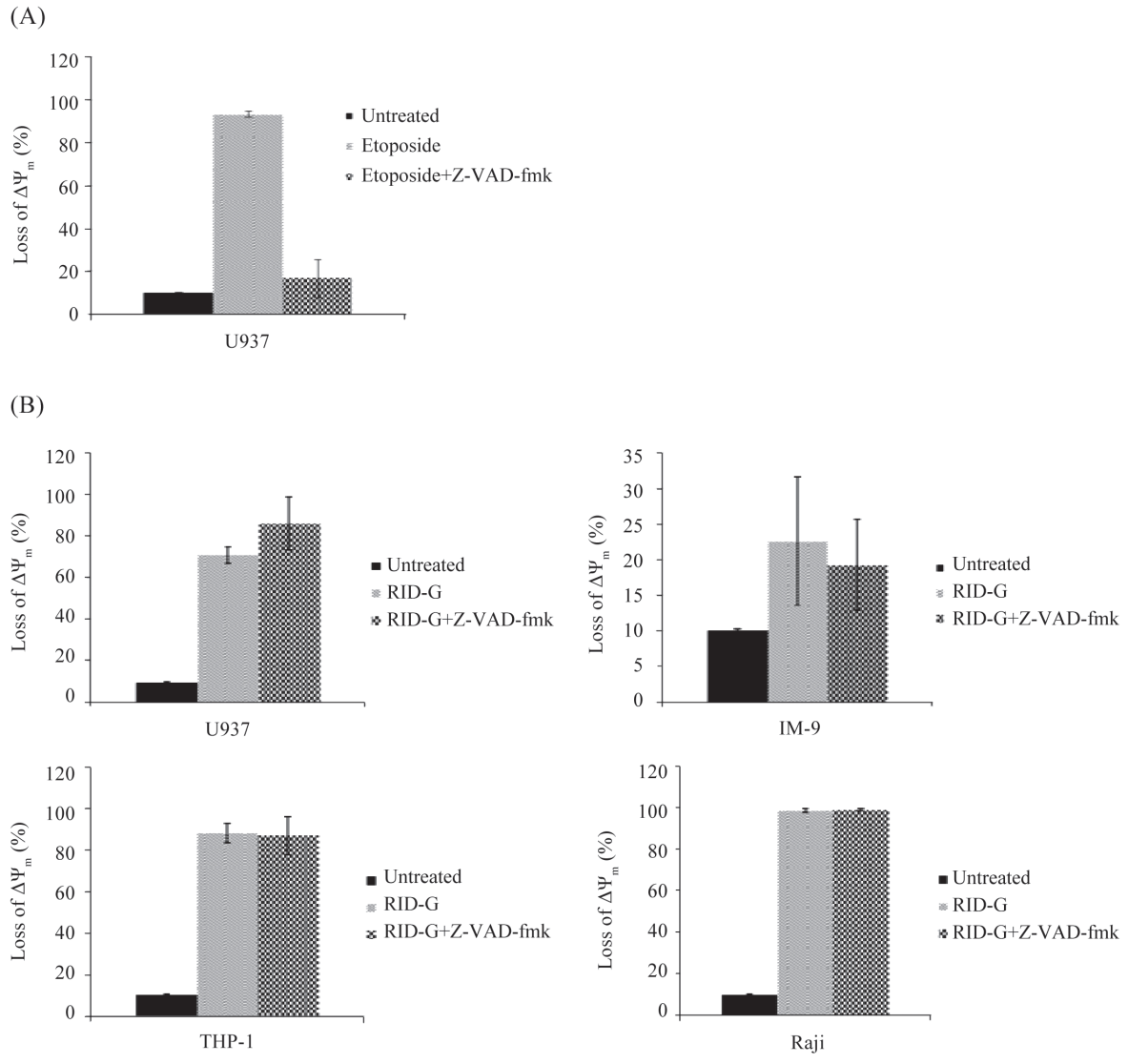

Fig.4 Effects of Z-VAD-fmk on RID-G or etoposide-induced loss of mitochondrial membrane potential ($\Delta\Psi_m$) determined by MitoTracker staining

RID-G, etoposide, and Z-VAD-fmk were used at final concentrations of 5 μmol/L, 5 μmol/L, and 20 μmol/L, respectively. The loss of $\Delta\Psi_m$ quantified by flow cytometric analysis after MitoTracker staining was measured at 6 h (RID-G) or 18 h (etoposide) after treatment. Data shown were means±SD from 3 independent experiments. A: Z-VAD-fmk suppresses etoposide-induced loss of $\Delta\Psi_m$ in U937 cells; B: Z-VAD-fmk can not suppress RID-G-induced loss of $\Delta\Psi_m$ in U937, IM-9, THP-1, and Raji cells.

70%~99% of cells lose their $\Delta\Psi_m$), and IM-9 cells were resistant to RID-G (only a 23% rise). Furthermore, these RID-G-induced mitochondrial changes were not suppressed by a pan-caspase inhibitor, Z-VAD-fmk (Fig.3B and Fig.4B), although Z-VAD-fmk suppressed etoposide-induced mitochondrial changes in U937 cells (Fig.3A and Fig.4A). These data indicate that RID-G, unlike etoposide, induces a caspase-independent mitochondrial dysfunction.

2.2 RID-G induces an early apoptotic change

To pursue the caspase-independent mechanism, we also analyzed the cells by Annexin V-FITC/PI double staining (Fig.5). The flow cytometric analysis detects the early apoptotic changes i.e., the cell-surface exposure of phosphatidylserine by FITC-labeled Annexin V. In conjunction with a dye exclusion

of PI, this analysis also discriminates intact cells ($FITC^-/PI^-$), early apoptotic cells ($FITC^+/PI^-$), and late apoptotic or necrotic cells ($FITC^+/PI^+$)[17]. In this analysis, RID-G predominantly induced a $FITC^+/PI^-$ early apoptotic change in all cell lines, suggesting that RID-G fundamentally elicit apoptotic signals, but not necrotic signals. Interestingly, the sensitivity of IM-9 cells to RID-G is comparable to the sensitivities of other cells in spite of their resistance to mitochondrial dysfunction. Again, Z-VAD-fmk failed to suppress RID-G-induced cell death (Fig.5B), although Z-VAD-fmk suppressed the etoposide-induced apoptosis in U937 cells (Fig.5A). These data further support our observations that the mode of action of RID-G is caspase-independent. We therefore speculate that RID-G induces a caspase-independent apoptosis in

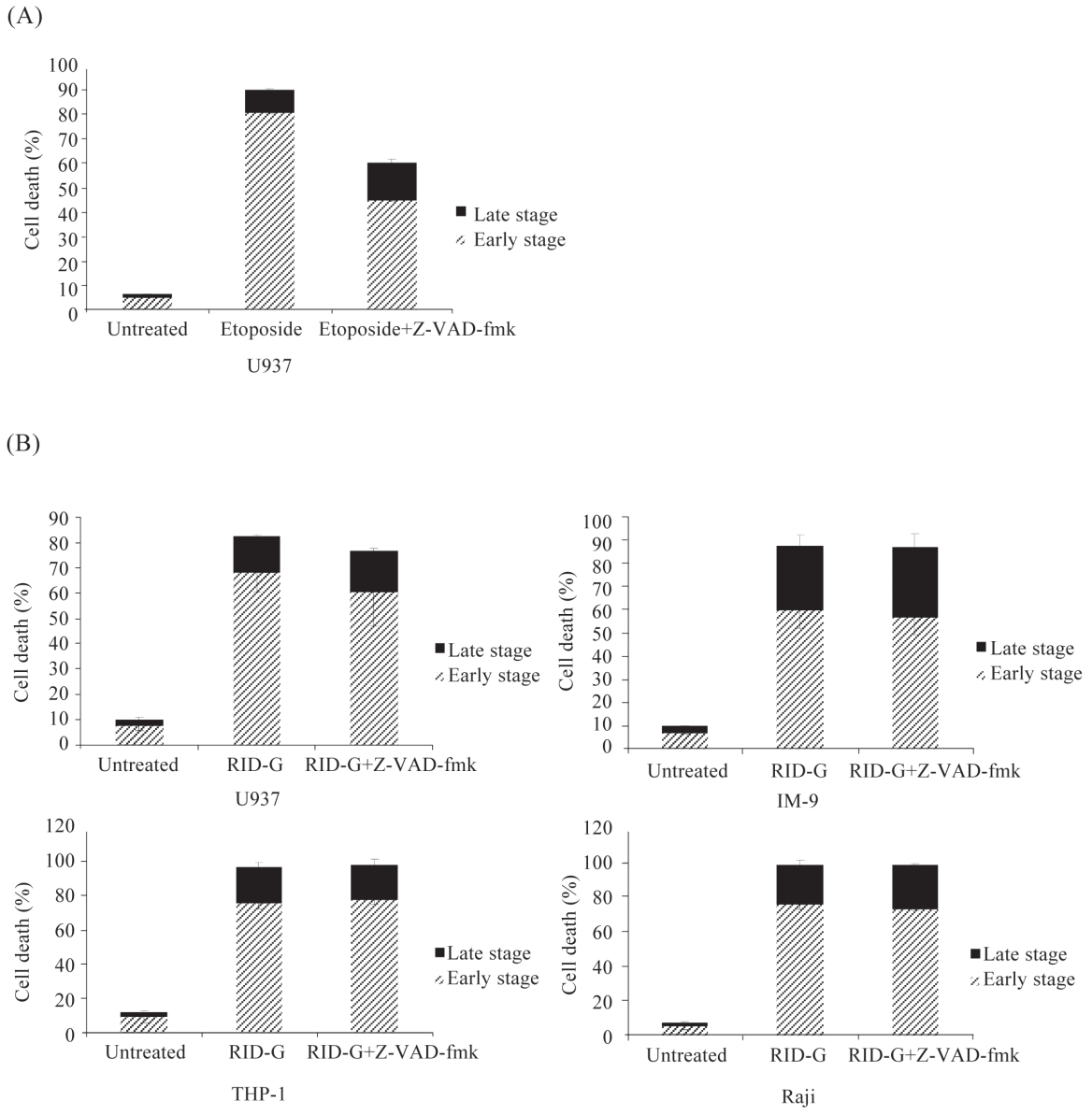

Fig.5 Effects of Z-VAD-fmk on RID-G or etoposide-induced cell death determined by Annexin V-FITC/PI double staining methods

RID-G, etoposide, and Z-VAD-fmk were used at final concentrations of 5 μmol/L, 5 μmol/L, and 20 μmol/L, respectively. The percentages of early and late cell death stages were determined at 6 h (RID-G) or 18 h (etoposide) after treatment. Early stage and late stage indicate $FITC^+/PI^-$ and $FITC^+/PI^+$ cells, respectively. Data shown were means±SD from 3 independent experiments. A: Z-VAD-fmk suppresses etoposide-induced cell death in U937 cells; B: Z-VAD-fmk cannot suppress RID-G-induced cell death in U937, IM-9, THP-1, and Raji cells.

these cells.

2.3 RID-G induces DNA fragmentation, but its pattern varies among cell lines

To further characterize RID-G-induced cell death is apoptosis or the other mode of cell death, we performed DNA fragmentation analysis in order to confirm whether the pattern of DNA fragmentation is the typical apoptotic "DNA ladder" or not. As shown in Figure 6, RID-G induced a DNA ladder formation in U937 cells, but the cells showed less DNA ladder formation than when treated with etoposide, and, surprisingly, RID-G induced smear of DNA fragmentations in Raji and THP-1 cells, suggesting that the cell death is not typical apoptosis. On the other hand, IM-9 cells did not show any DNA fragmentation 6 h after RID-G treatment, possibly by their resistance to mitochondrial dysfunction (data not shown). Furthermore, Z-VAD-fmk showed inconsistent effects on these DNA fragmentations: it largely suppressed, partialy suppressed, and on the contrary, enhanced DNA fragmentaion in U937, THP-1, and Raji cells, respectively. These results suggest that the machinery for typical caspase-dependent apoptotic DNA fragmentation is partially activated in RID-G-treated U937 cells, and that typical DNA degradations occur in a caspase-dependent and a caspase-suppressible manner in THP-1 and Raji cells, respectively.

Taken together, Table 1 shows a summary of effects of Z-VAD-fmk on RID-G or etoposide-induced cell death in U937 cells. These data indicate that RID-G mainly induces caspase-independent cell death accompanied with mitochondrial dysfunction, and the

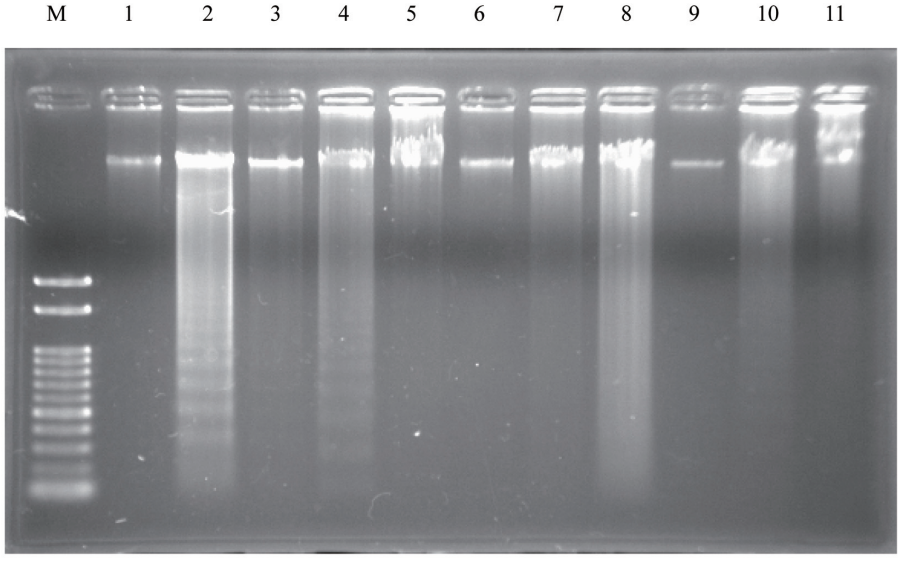

Fig.6 Effects of Z-VAD-fmk on RID-G or etoposide-induced cell death detected by DNA ladder formation

RID-G, etoposide, and Z-VAD-fmk were used at final concentrations of 5 μmol/L, 5 μmol/L, and 20 μmol/L, respectively. The DNA ladder formation was detected by agarose gel electrophoresis. Cells were harvested at 6 h (RID-G) or 18 h (etoposide) after treatment. M: 100 bp ladder marker; lane 1: untreated U937; lane 2: etoposide-treated U937; lane 3: etoposide + Z-VAD-fmk-treated U937; lane 4: RID-G-treated U937; lane 5: RID-G + Z-VAD-fmk-treated U937; lane 6: untreated Raji; lane 7: RID-G-treated Raji; lane 8: RID-G + Z-VAD-fmk-treated Raji; lane 9: untreated THP-1; lane 10: RID-G-treated THP-1; lane 11: RID-G + Z-VAD-fmk-treated THP-1.

Table 1 Summary of effects of Z-VAD-fmk on RID-G or etoposide-induced cell death in U937 cells

Groups	RID-G	RID-G+Z-VAD-fmk	Etoposide	Etoposide+Z-VAD-fmk
MTT assay	+	+	+	-
MitoTracker	+	+	+	-
Annexin V-FITC/PI	+	+	+	-
DNA ladder	+	-	++	-

+: cell death is induced; ++: cell death is more strongly induced than RID-G treatment; -: cell death is suppressed.

late apoptotic event such as DNA fragmentation is mediated by caspases in some cell lines.

3 Discussion

In the present study, we showed that RID-G mainly induces caspase-independent cell death accompanied by mitochondrial dysfunction in four neoplastic hematopoietic cell lines, U937, Raji, THP-1, and IM-9 cells, and that the patterns of RID-G-induced DNA fragmentations are different among cell lines through the mechanisms that can not be explained by the classical caspase-dependent mechanism alone.

Mitochondrion is the key factor involved in apoptosis; the current view is that the mitochondrion is not only an initiator of apoptosis, but also an amplifier of apoptotic signals. The important feature of apoptosis is a permeability change in the mitochondrial membrane, which is the central link in the general apoptotic pathway. The mitochondrial outer membrane permeabilization leads to the release of a variety of apoptogenic proteins such as Cyt *c*[2,18,19], second mitochondria-derived activator of caspase/direct IAP-binding protein with low PI (Smac/Diablo)[20~23], Omi/HtrA2[24,25], apoptosis inducing factor (AIF)[26], and endonuclease G (EndoG)[27] from mitochondria into cytosol, resulting in the mitochondrial dysfunction including the loss of $\Delta\Psi_m$ and the uncoupling of the respiratory chain.

During these mitochondrial changes, caspases play a role in enhancing the mitochondrial disruption through cleavages of some Bcl-2 family proteins such as Bcl-2, Bcl-xL, and Bid. The irreversible cleavages can switch them from anti- to pro-apoptotic property in Bcl-2 and Bcl-xL[28~30], and convert Bid from mildly to strongly apoptotic[5,31], which are considered as a possible cause of the effectiveness of Z-VAD-fmk in suppressing etoposide-induced mitochondrial dysfunction in U937 cells (Fig.3A and Fig.4A). On the other hand, Z-VAD-fmk did not show any inhibitory activity against RID-G-induced mitochondrial dysfunction (Fig.3B and Fig.4B). The results indicate that the caspase-mediated enhancement is dispensable for RID-G-induced mitochondrial dysfunction, which could be explained solely by an initial damage by RID-G alone due to its strong ability to impair mitochondria. This would also raise the possibility that the damage is too excessive to prevent death such as necrosis. However, RID-G-induced death is probably not necrosis, because the death exhibited an early apoptotic change in the flow cytometric analysis using Annexin V-FITC/PI double staining (Fig.5). Explorations of the target molecules of RID-G may provide new insight into the intracellular mechanisms of cell death.

In DNA fragmentation analysis, the pattern of RID-G-induced DNA fragmentation and the response of the fragmentation to Z-VAD-fmk varied among cell lines (Fig.6). The fact that these RID-G-treated cells died regardless of the presence or absence of Z-VAD-fmk as assessed by three different methods (Fig.3~Fig.5) indicates that the suppressions of DNA fragmentation by Z-VAD-fmk in U937 and THP-1 cells does not mean the recovery from the death, but merely mean the mechanistic inhibition of the final step(s) of the cell death. The fragmentation of DNA into nucleosomal units is caused by an enzyme known as caspase activated DNase (CAD). Normally, CAD exists as an inactive complex with ICAD (inhibitor of CAD). During apoptosis, ICAD is cleaved by caspases such as caspase-3, to release CAD, followed by rapid internucleosomal fragmentation of the nuclear DNA[32,33]. The culprit of the DNA fragmentation could be CAD and/or CAD-like nuclease, because the fragmentation is a typical “DNA ladder” and inhibited by Z-VAD-fmk, which indicates that the responsible nuclease is a caspase-dependent one that cause internucleosomal DNA fragmentation. In contrast, the responsible nuclease(s) in THP-1 and Raji cells are considered not to be CAD, since the fragmentation in these cells is a smear of DNA fragmentation. Considering the strong activity of RID-G against mitochondria, the nucleases in THP-1 and Raji cells may be other nuclear DNA degrading factors released from the mitochondria, e.g., EndoG and AIF, although

how caspases involved in these DNA fragmentations in THP-1 and Raji cells is unclear. Especially, EndoG is reported to induce a smear of DNA fragmentation[34]. This hypothesis further supported by our observation that the RID-G-resistant cell line, IM-9 cells, showed a resistance to DNA fragmentation (data not shown) as well as mitochondrial dysfunction (Fig.3 and Fig.4).

Taken together, RID-G has a strong cell death-inducing activity, and may induce a novel mode of cell death. RID-G may serve to develop a new type of anticancer drugs. The modes of cell death are recently classified into several modes including apoptosis, necrosis, autophagy, mitotic catastrophe, and so on[35,36]. Further investigations are warranted to determine whether RID-G-induced cell death can be classified into one of those classifications or not.

References

1 Zamzami N, Marzo I, Susin SA, Brenner C, Larochette N, Marchetti P, *et al*. The thiol crosslinking agent diamide overcomes the apoptosis-inhibitory effect of Bcl-2 by enforcing mitochondrial permeability transition. Oncogene 1998; 16(8): 1055-63.

2 Liu XS, Kim CN, Yang J, Jemmerson R, Wang XD. Induction of apoptotic program in cell-free extracts: requirement for dATP and cytochrome *c*. Cell 1996; 86(1): 147-57.

3 Narita M, Shimizu S, Ito T, Chittenden T, Lutz RJ, Matsuda H, *et al*. Bax interacts with the permeability transition pore to induce permeability transition and cytochrome *c* release inisolated mitochondria. Proc Natl Acad Sci USA 1998; 95(25): 14681-6.

4 Zha J, Harada H, Osipov K, Jockel J, Waksman G, Korsmeyer SJ. BH_3 domain of BAD is required for heterodimerization with Bcl-xL and proapoptotic activity. J Biol Chem 1997; 272(39): 24101-4.

5 Luo X, Budihardjo I, Zou H, Slaughter C, Wang X. Bid, a Bcl2 interacting protein, mediates cytochrome *c* release from mitochondria in response toactivation of cell surface death receptors. Cell 1998; 94(4): 481-90.

6 Li P, Nijhawan D, Budihardjo I, Srinivasula SM, Ahmad M, Alnemri ES, *et al*. Cytochrome *c* and dATP-dependent formation of Apaf-1/caspase-9 complex initiates an apoptotic protease cascade. Cell 1997; 91(4): 479-89.

7 Mandlekar S, Yu R, Tan TH, Kong AN. Activation of caspase-3 and c-JunNH_2-terminal kinase-1 signaling pathways in tamoxifen-induced apoptosis of human breast cancer cells. Cancer Res 2000; 60(21): 5995-6000.

8 Ferlini C, Scambia G, Marone M, Distefano M, Gaggini C, Ferrandina G, *et al*. Tamoxifen induces oxidative stress and apoptosis in oestrogen receptor-negative human cancer cell lines. Br J Cancer 1999; 79(2): 257-63.

9 Nagahara Y, Shinna I, Nakata K, Sasaki A, Miyamoto T, Ikekita M. Induction of mitochondria-involved apoptosis in estrogen receptor-negative cells by a novel tamoxifen derivative, ridaifen-B. Cancer Sci 2008; 99(3): 608-14.

10 Shiina I, Suzuki M, Yokoyama K. Short-step synthesis of tamoxifen and its derivatives via the three-component coupling reaction and migration of the double bond. Tetrahedron Lett 2004; 45(5): 965-7.

11 Shiina I, Sano Y, Nakata K, Kikuchi T, Sasaki A, Ikekita M, *et al*. Synthesis of the new pseudo-symmetrical tamoxifen derivatives and their anti-tumor activity. Bioorg Med Chem Lett 2007; 38(36): 2421-4.

12 Shiina I, Sano Y, Nakata K, Suzuki M, Yokoyama T, Sasaki A, *et al*. An expeditious synthesis of tamoxifen, a representative SERM (selective estrogen receptor modulator), via the three-component coupling reaction among aromatic aldehyde, cinnamyltrimethylsilane, and β-chlorophenetole. Bioorg Med Chem 2007; 15(24): 7599-617.

13 Shiina I, Sano Y, Nakata K, Kikuchi T, Sasaki A, Ikekita M, *et al*. Synthesis and pharmacological evaluation of the novel pseudo-symmetrical tamoxifen derivatives as anti-tumor agents. Biochem Pharm 2008; 75(5): 1014-26.

14 Alley MC, Scudiero DA, Monks A, Hursey ML, Czerwinski MJ, Fine DL, *et al*. Feasibility of drug screening with panels of human tumor cell lines using a microculture tetrazolium assay. Cancer Res 1988; 48(3): 589-601.

15 Nakai J, Kawada K, Nagata S, Kuramochi K, Uchiro H, Kobayashi S, *et al*. A novel lipid compound, epolactaene, induces apoptosis: Its action is modulated by its side chain structure. Biochim Biophys Acta 2002; 1581(1-2): 1-10.

16 Morita A, Zhu J, Suzuki N, Enomoto A, Matsumoto Y, Tomita M, *et al*. Sodium orthovanadate supprese DNA damage-induced caspase activation and apoptosis by inactivating p53. Cell Death Differ 2006; 13(3): 499-511.

17 Vermes I, Haanen C, Steffens-Nakken H, Reutelingsperger C. A novel assay for apoptosis. Flow cytometric detection of phosphatidylserine expression on early apoptotic cells using fluorescein labelled annexin V. J Immunol Methods 1995; 184(1): 39-51.

18 Kluck RM, Wetzel EB, Green DR, Newmwyer DD. The release of cytochrome *c* from mitochondria: A primary site for Bcl-2 regulation of apoptosis. Science 1997; 275(5303): 1132-6.

19 Yang J, Liu XS, Bhalla K, Kim CN, Ibrabo AM, Cai JY, *et al*. Prevention of apoptosis by Bcl-2: Release of cytochrome *c* from mitochondria blocked. Science 1997; 275(5303): 1129-32.

20 Du CY, Fang M, Li YC, Li LY, Wang XD. Smac, a mitochondrial protein that promotes cytochrome *c*-dependent caspase activation by elimination IAP inhibition. Cell 2000; 102(1): 33-42.

21 Verhagen AM, Ekert PG, Pakusch M, Silke J, Connolly LM, Reid GE, *et al*. Identification of DIABLO, a mammalian protein that

promotes apoptosis by binding to and antagonizing IAP proteins. Cell 2000; 102(1): 43-53.
22 Liu Z, Sun C, Olejinicazak ET, Meadows RP, Betz SF, Oost T, *et al*. Structural basis for binding of Smac/DIABLO to the XIAP BIR3 domain. Nature 2000; 408(6815): 1004-8.
23 Wu G, Chai JJ, Suber TL, Wu JW, Du CY, Wang XD, *et al*. Structural basis of IAP recognition by Smac/DIABLO. Nature 2000; 408(6815): 1008-12.
24 Hegde R, Srinivasula SM, Zhang ZJ, Wassell R, Mukattash R, Cilenti L, *et al*. Identification of Omi/HtrA2 as a mitochondrial apoptotic serine protease ehat disrupts inhibitor of apoptosis protein-caspase interaction. J Biol Chem 2002; 277(1): 432-8.
25 Martins LM, Iaccarino I, Tenev T, Gschmeissner S, Totty NF, Lemoine NR, *et al*. The serine protease Omi/HtrA2 regulates apoptosis binding XIAP through a reaper-like motif. J Biol Chem 2002; 277(1): 439-44.
26 Susin SA, Lorezo HK, Zamzami N, Marzo I, Snow BE, Brothers GM, *et al*. Molecular characterization of mitochondrial apoptosis-inducing factor. Nature 1999; 397(6718): 441-6.
27 Li LY, Luo X, Wang XD. Endonuclease G is an apoptotic DNase when released from mitochondria. Nature 2001; 412(6842): 95-9.
28 Cheng EH, Kirsch DG, Clem RJ, Ravi R, Kastan MB, Bedi A, *et al*. Conversion of Bcl-2 to a Bax-like death effector by caspase. Science 1997; 278(5345): 1966-8.
29 Clem RJ, Cheng EH, Karp CL, Kirsch DG, Ueno K, Takahashi A, *et al*. Modulation of cell death by Bcl-xL through caspase interaction. Proc Natl Acad Sci USA 1998; 95(2): 554-9.
30 Bellows DS, Chau BN, Lee P, Lazebnik Y, Bums WH, Hardwick JM. Antiapoptotic herpesvirus Bcl-2 homologs escape caspase-mediated conversion to proapoptotic proteins. J Virol 2000; 74(11): 5024-31.
31 Li H, Zhu H, Xu CJ, Yuan J. Cleavage of BID by caspase 8 mediates the mitochondrial damage in the Fas pathway of apoptosis. Cell 1998; 94(4): 491-501.
32 Enari M, Sakahira H, Yokoyama H, Okawa K, Iwamatsu A, Nagata S. A caspase-activated DNase that degrades DNA during apoptosis, and its inhibitor ICAD. Nature 1998; 391(6662): 43-50.
33 Sakahira H, Enari M, Nagata S. Cleavage of CAD inhibitor in CAD activation and DNA degradation during apoptosis. Nature 1998; 391(6662): 96-9.
34 Loo GV, Schotte P, Gurp MV, Demol H, Hoorelbeke B, Gevaert K, *et al*. Endonuclease G: A mitochondrial protein released in apoptosis and involved in caspase-independent DNA degradation. Cell Death Differ 2001; 8(12): 1136-42.
35 Kroemer G, Galluzzi L, Vandenabeele P, Abrams J, Alnemri ES, Baehrecke EH, *et al*. Classification of cell death: Recommendations of the nomenclature committee on cell death 2009. Cell Death Differ 2009; 16(1): 3-11.
36 Galluzzi L, Maiuri MC, Vitale I, Zischka H, Castedo M, Zitvogel L, *et al*. Cell death modalities: Classification and pathophysiological implications. Cell Death Differ 2007; 14(7): 1237-43.

Ridaifen-G诱导细胞死亡不依赖于细胞凋亡蛋白酶

安里菲热·安尼瓦尔[1,2] 羽鸟麻奈美[2] 森田明典[2] 椎名勇[3]
中田健也[3] 户崎雄太[3] 王艳雯[3] 池北雅彦[2] 李 冠[1]*
([1]新疆大学生命科学与技术学院, 乌鲁木齐 830046; [2]东京理科大学理工学部应用生物科学科, 千叶县 278-8510;
[3]东京理科大学理学部应用化学科, 东京 162-8601)

摘要 通过对Ridaifen-G(RID-G)诱导造血细胞U937、Raji、THP-1和IM-9死亡是否需要Z-VAD-fmk(一种细胞凋亡蛋白酶抑制剂)的研究, 发现RID-G以细胞凋亡蛋白酶非依存性的方式诱导细胞死亡, 并伴随有线粒体功能紊乱。Z-VAD-fmk对U937细胞的死亡没有影响, 但抑制etoposide诱导的细胞凋亡; DNA片段化结果表明, RID-G可破坏Raji和THP-1细胞的DNA, 经RID-G处理后的U937细胞的DNA条带没有经etoposide处理的清晰。此外, Z-VAD-fmk对U937、THP-1和Raji细胞DNA的片段化程度有不同的影响, 抑制细胞死亡。这些结果表明, RID-G诱导的非典型细胞死亡不依赖于caspase, 且伴随有线粒体功能紊乱。

关键词 细胞死亡; 线粒体; 细胞凋亡蛋白酶; 细胞凋亡; Ridaifen-G

收稿日期: 2011-01-19 接受日期: 2011-03-03
*通讯作者。Tel: 0991-8581106, E-mail: guanli@xju.edu.cn